Journal of Neuroscience Methods 391 (2023) 109850

Contents lists available at ScienceDirect

Journal of Neuroscience Methods

journal homepage: www.elsevier.com/locate/jneumeth

Recording central nervous system responses of freely-swimming marine and freshwater fishes with a customizable, implantable AC differential amplifier

Brendan J. Gibbs, James A. Strother, James C. Liao *

Department of Biology/ The Whitney Laboratory for Marine Bioscience, University of Florida, United States

ARTICLE INFO

Keywords:
Brain recording
Printable circuit board
Fishes
Hydrodynamic

ABSTRACT

Background: Fish have adapted to a diversity of environments but the neural mechanisms underlying natural aquatic behaviors are not well known.
New method: We have developed a small, customizable AC differential amplifier and surgical procedures for recording multi-unit extracellular signals in the CNS of marine and freshwater fishes.
Results: Our minimally invasive amplifier allowed fish to orient to flow and respond to hydrodynamic and visual stimuli. We recorded activity in the cerebellum and optic tectum during these behaviors.
Comparison with existing methods: Our system is very low-cost, hydrodynamically streamlined, and capable of high-gain in order to allow for recordings from freely behaving, fast fishes in complex fluid environments.
Conclusions: Our tethered approach allows access to record neural activity in a diversity of adult fishes in the lab, but can also be modified for data logging in the field.

1. Introduction

Any mechanistic understanding of animal behavior requires insight into the neural activity of the brain. Neural recordings in the brain have traditionally involved rigid mounting of the head to remove motion artifacts that can obscure small neuronal signals. While this approach has provided insights into fundamental mechanisms of neural processing (Evarts, 1968; Turner and DeLong, 2000), some of the most recent exciting discoveries have been in freely moving animals (Yartsev and Ulanovsky, 2013; Musall et al., 2019; Rynes et al., 2021). These studies have taught us that neurons behave in profoundly different ways when an animal moves and interacts with its environment compared to when it is immobilized. These changes are particularly pronounced in sensory processing regions, as sensory input must be integrated with an animal's own movement to provide an accurate representation of a complex and unpredictable external environment. (Crapse and Sommer, 2008; Skandalis et al., 2021; Philip et al., 2020). Revealing the neural basis of movement behaviors, which have evolved in nature, therefore depends on recording from freely moving animals free from experimental stress (Girotti et al., 2006; Juczewski et al., 2020; Rynes et al., 2021).

With over 34,000 species, fishes are the most speciose group of vertebrates and have evolved behaviors that have allowed them to radiate into a tremendous diversity of ecological habitats. As a model system, fishes have also played a key role in understanding critical neural processes ranging from the mechanisms of the voltage gated Na+ channel (Agnew et al., 1978; Noda et al., 1984; Catterall, 1988) to the color-coding abilities of retinal neurons (Daw, 1968). More recently, the larval zebrafish system has opened up powerful optogenetic approaches to examine whole-brain activity in fixed and even freely moving individuals (Ahrens et al., 2013; Kim et al., 2017). Still, optogenetic methods requires tissue transparency and is thus limited to the larval stage, during which many behaviors are still developing. The brain activity of adult fishes is currently much more challenging to investigate. Even though the neural architecture of fishes suggests a level of behavioral sophistication approaching mammals (Broglio et al., 2003; Brown et al., 2006), only a few studies have recorded neural activity from freely swimming fishes (Palmer et al., 2003; Canfield and Mizumori, 2004; Weiss et al., 2006; Vinepinksy et al., 2017; Takahashi et al., 2021). Wireless recordings of brain activity from a freely swimming goldfish (*Carassius auratus*) showed that neural activity in the telencephalon was correlated with swimming speed and a specific heading vector (Vinepinksy et al., 2020). This pioneering approach is not trivial to develop, as a small, waterproof housing is needed to prevent water from leaking into sensitive electronics (Vinepinksy et al., 2017;

* Corresponding author.
E-mail address: jliao@whitney.ufl.edu (J.C. Liao).

https://doi.org/10.1016/j.jneumeth.2023.109850
Received 6 December 2022; Received in revised form 23 March 2023; Accepted 2 April 2023
Available online 5 April 2023

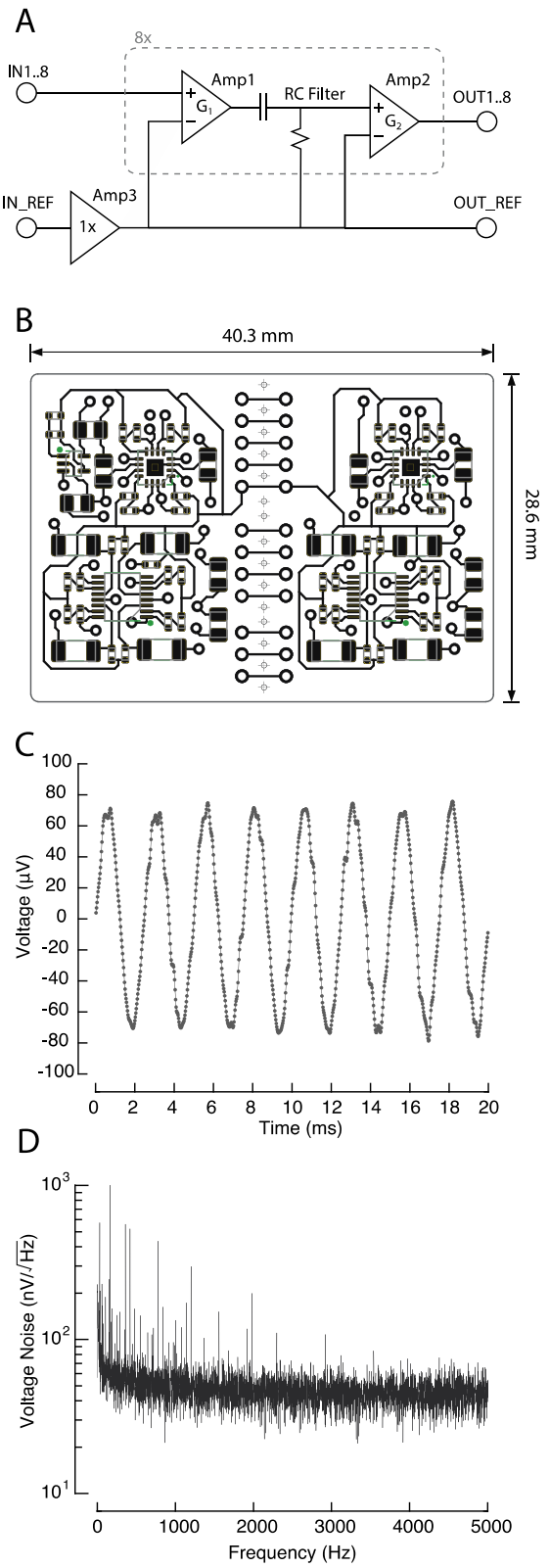

Fig. 1. (A) Schematic diagram of the custom-developed amplifier used in this study. (B) Layout of the printed circuit for the amplifier (represented by top copper plane). (C) Recording of a sine wave 150 μV p-p test signal (10,000x total gain, 300–5000 Hz filter, 40 ksps), showing that noise is modest and the signal is well-resolved. (D) Spectral density of input voltage noise (10,000x total gain, 1–20,000 Hz filter, 40 ksps).

Takahashi et al., 2021). While electrophysiology systems can be waterproofed and adapted from terrestrial animals like rats, the high cost can be prohibitive. Additionally, the housings used in previous fish studies are not streamlined in shape, which limits a wide range of natural movements, especially for species that are fast-swimming or live in current-swept environments. Our initial efforts to measure potentials from freely-swimming fishes using a traditional desktop amplifier yielded noisy recordings, likely due to the long wires picking up environmental electromagnetic noise. Subsequent efforts using a commercially available headstage were also unsuccessful, as the amplifier was difficult to waterproof, and appeared to be easily destroyed by electrostatic discharge (ESD), and was costly to replace when damaged (>$1500). Here, we set out to design and implement a neural recording amplifier that is both hydrodynamically streamlined and cost effective to encourage comparative neural recordings in adult fishes.

2. Methods

2.1. Overview

We designed a tethered, experimental setup to record real-time neural activity from the brains of fresh and saltwater fishes as they freely behave. We chose the freshwater rainbow trout (*Oncorhynchus mykiss*) and saltwater oyster toadfish (*Opsanus tau*) to demonstrate our results. At the core of our system is a small, modular AC differential amplifier custom-designed for electrophysiological recordings in water (Fig. 1). The amplifier provides multiple independent channels, which allows electrode arrays to be implanted into the brain. A small (length=163 cm; diameter=3 mm) output cable was connected to a differential AC amplifier (Fig. 2). Our system can also be configured with a data logger to permit wireless recordings.

2.2. AC differential amplifier

We constructed an amplifier which is a high-input impedance two-stage amplifier (Prutchi and Norris, 2005). The first stage consists of a low-noise JFET-input (junction-gate field-effect transistor) operational amplifier (op-amp) configured for non-inverting gain. The JFET input provides low input bias currents (<1 pA) and is far more resistant to ESD (electrostatic discharge) damage than a MOSFET (metal–oxide–semiconductor field-effect transistor) input (Schreier, 1978). The output from the first stage is passed through a simple RC filter that removes DC signals produced by electrode polarization and the input offset voltage of the op-amp, which would saturate subsequent stages if not removed. This signal is further amplified in a second stage CMOS (complementary metal-oxide-semiconductor) op-amp operating in a non-inverting configuration. This second stage also functions as the output cable driver, and parasitic oscillations that may be induced by cable capacitance are suppressed by the low loop gain of the non-inverting configuration and selecting op-amps that are intrinsically robust to output capacitance (C-Load™). In order to reject stray common potentials, all input signals are differentially amplified by subtracting off a reference input. This reference input is buffered using a unity-gain amplifier, which provides a low-impedance signal for subsequent stages and provides a common mode rejection ratio (CMRR) limited only by the CMRR of the op-amp, which is usually exceptional (here, 90 dB typical). Unity-gain configurations can be less stable, and parasitic oscillations are suppressed using a resistor-capacitor feedback network and selection of a nominally unity-gain stable op-amp. Low power components were used for all integrated circuits (IC) to enable this amplifier to be readily adapted for battery-powered applications.

The head stage amplifier was implemented with 8-channels using surface mount components on a 4-layer printed circuit board (40.3 mm × 28.6 mm). The board was designed with an interconnect through the midline, such that the board can be cut in half to produce a smaller 4-channel amplifier, or the board can be folded along this

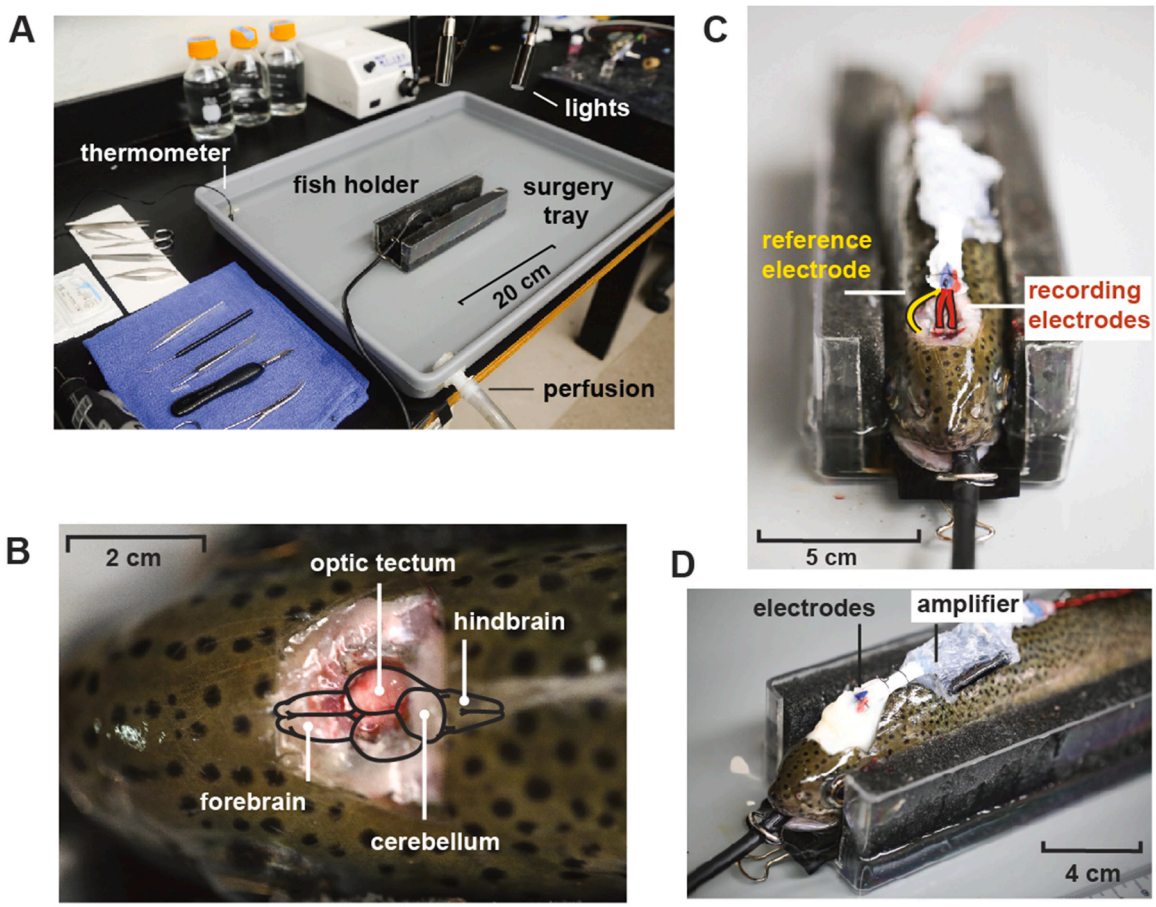

Fig. 2. (A) Surgical setup with perfusion system and fish holder. (B) Exposed trout brain after skin and bone removal. (C) Insertion of recording electrodes (position indicated by drawn red line) into the cerebellum and the reference electrode (position indicated by yellow line) into the cerebral spinal fluid. (D) After electrode implantation, the cranial cavity was sealed with dental cement to lock electrodes in place.

midline to produce a smaller 8-channel amplifier (20.1 × 28.6 mm) by using a flex board cutting and rejoining a rigid board.

A major advantage of using a custom circuit is the ability to readily modify the design for different applications. The gain of the first stage is given by

$$G_1 = 1 + R_5/R_1$$

where G_1 is the gain of the amplifier, and R_1 and R_5 are resistor values. In our implementation, these resistors were selected to produce a gain of 50x ($R_1 = 10.2\ k\Omega$, $R_5 = 499\ k\Omega$), which was sufficient to reduce the effects of noise of subsequent stages while avoiding input saturation. The cutoff frequency of the RC filter is

$$f_c = \frac{1}{2\pi R_{11} C_5}$$

where f_c is the cut-off frequency, and R_{11} and C_5 are resistor and capacitor values. We selected values to produce a cutoff frequency of 2 Hz ($R_{11} = 1.18\ M\Omega$, $C_5 = 68nF$). Lastly, the gain of the second stage is

$$G_2 = 1 + R_9/R_{10}$$

where G_2 is the gain of the amplifier, and R_9 and R_{10} are resistor values. For our experiments, our amplifier was configured with a gain of 2x ($R_9 = 4.7\ k\Omega$, $R_{10} = 4.7\ k\Omega$). When used in conjunction with a desktop amplifier, this amounted to a total gain of 100x. However, the amplifier can be easily configured for other gain or filter values simply by selecting different resistor and capacitor values, which allows this amplifier to be used in a broad range of applications, including wireless configurations.

Although the amplifier may be configured to interface directly with a data acquisition system, in this case it was convenient to condition the output using a desktop extracellular differential amplifier (Model 1700, AM Systems, Sequim, WA, USA). Signals were then recorded using an analog to digital converter (Powerlab 16/35, AD Instruments Ltd, Dunedin, NZ).

The performance of the system was subsequently verified. Microvolt test signals were generated by scaling a signal from a function generator using a resistive voltage divider (1/1000x), and then amplified outputs were recorded and compared to the input (Fig. 1C). Similarly, the input voltage noise was determined by grounding the inputs and recording the amplified output (Fig. 1D). The measured noise spectrum showed low noise levels, with a typical combination of 1/f and white noise.

It was not uncommon for minor technical issues to arise during experimental trials, such as loose connections or broken wires. Often these issues were not obvious and only apparent after a trial failed to produce robust responses. To eliminate such problems, a small test board was produced that directly connected to the inputs of our amplifier, and which allowed the verification tests described above to be performed prior to each trial.

Note that detailed schematics of the circuit board files are found in the supplementary information. This includes industry-standard gerber files which can be supplied to any printed circuit board manufacturer to produce the amplifier and test board in this study.

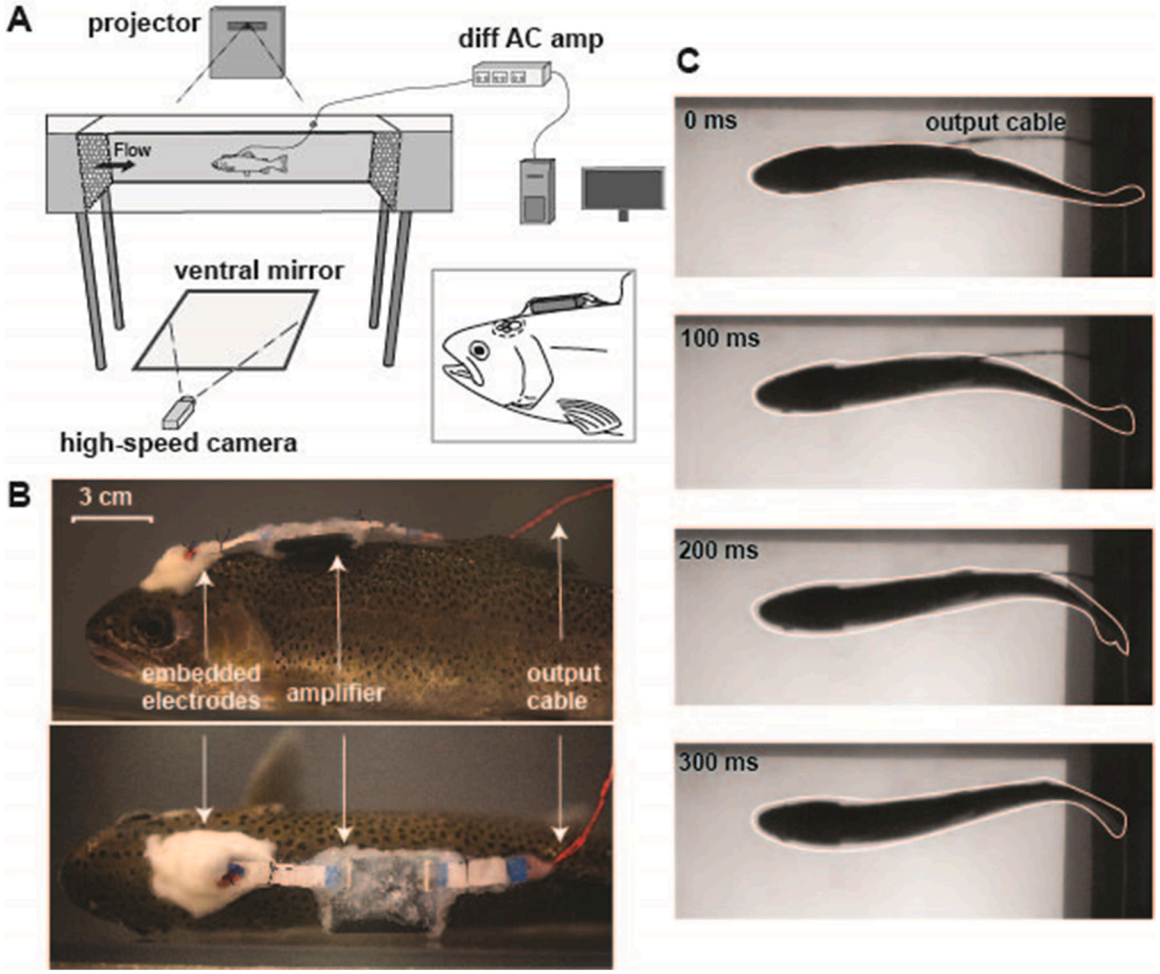

Fig. 3. Experimental Overview (A) Brain activity was observed as fish swam in a flow tank. A projector mounted over the working section of the tank provided visual stimuli and a high-speed camera recorded swimming kinematics. (B) Our low-profile amplifier allows for naturalistic swimming in different flows. (C) A stereotypical swimming sequence in flow with our tethered recording configuration.

2.3. Electrode and output cable fabrication

Homemade polyimide insulated tungsten electrodes (35 μm, California Fine Wire Company, CA, USA) were used to record multi-unit extracellular signals from the brain. Electrodes were cut to length (~2.5 cm) and the ends of each wire were burned with a lighter to remove the polyimide insulation. Electrode tips were soaked overnight in propanol to remove any residue from the burning process. Once clean, one end of the electrode wire was soldered to a 10-channel ribbon jumper (FFC flex cable jumper, Molex, Ill, USA) under a dissecting microscope (Stemi 2000-C, Zeiss, Germany). Electrode connectivity with the ribbon jumper was checked using a multimeter (2708B, B&K Precision, CA, USA).

The output cable was fabricated in similar fashion to the electrodes. Polyurethane enameled copper wires (30 AWG, Bntechgo, CA, USA) were cut to length (163 cm) and the enamel was removed with a scalpel from the wire ends. The end of each wire was soldered to its corresponding pad on a 12-channel ribbon jumper (FFC flex cable jumper, Molex, Ill, USA) under a dissecting microscope. The other end of the wire was then soldered to wires of a DB 25-pin female connector (Uxcell, Hong Kong, China). The female connector interfaced with a 25-pin male connector (Uxcell, Hong Kong, China) wired to the external power source (AA battery holder, OSEPP electronics, AZ, USA) and a differential AC amplifier (Model 1700, AM Systems, Sequim, WA, USA). Output cable wires were braided together to form a single wire.

2.4. Waterproofing

After our amplifier was checked with the test board, the entire circuit board, excluding the two connectors (FFC connector, Hirose Electric Co Ltd, Japan), was covered in slow curing epoxy (DP 270 Black, 3 M, MN, USA). Ribbon jumper pads interfacing with the electrodes and output cable were covered in 5-minute curing epoxy (The Gorilla Glue Company, OH, USA). The ribbon jumpers for the electrodes and output cable were then attached to their corresponding connector on the amplifier. The area was covered with all-purpose silicone (General Electric, MA, USA) and allowed to dry overnight. After experimentation concluded, the silicone was removed from the connectors with a scalpel. This allowed the amplifier and output cable to be reused so that only the electrodes would have to be refabricated for each experiment.

2.5. Surgery and implantation

Adult rainbow trout were obtained from a commercial hatchery (Wolf Creek National Fish Hatchery, Jamestown, KY, USA). Fish were held in a 500 L freshwater tank (maintained at 15 ± 1 °C) with a constant flow and were fed commercial trout pellets daily. Five trout (BL=29.1 ± 0.44 cm) were used in our experiments.

Wild oyster toadfish were collected by hook and line in the St. Augustine Inlet. Toadfish were held in a 750 L flow-through saltwater tank and were fed live shrimp daily. Seven toadfish (BL=29.4 ± 3.1 cm) were used in our experiments.

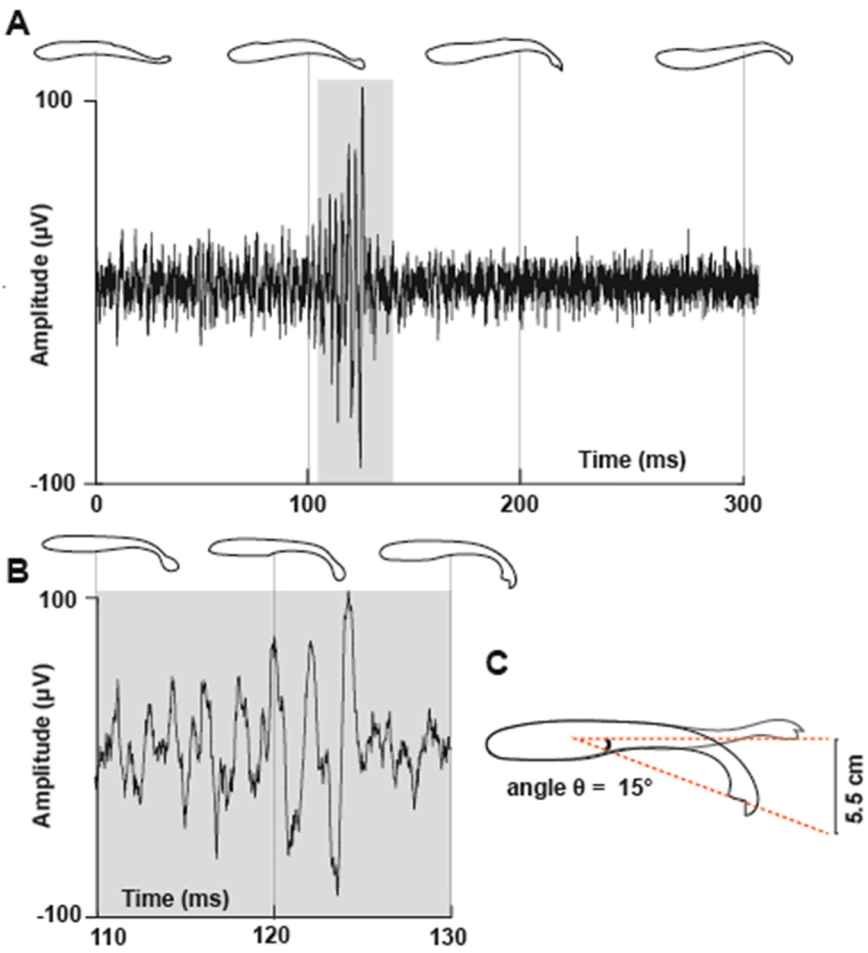

Fig. 4. Multi-unit extracellular recording from the cerebellum of a rainbow trout swimming in flow (0.94 Ls^{-1}). (A) Illustrated whole-body kinematics from a swimming sequence are shown above cerebellar recording (images correspond to Fig. 3C). (B) Expanded region of cerebellar activity in A, along with corresponding body kinematics. (C) Tailbeat displacement and the angle of the tail (θ) relative to the center of mass during this swimming sequence, corresponding to time sequence 0–200 ms in A.

Trout were anesthetized in 2.6 L tank (15 ± 1 °C) containing a solution of 0.0409 g l-1 tricaine methanesulfonate (MS-222; Finquel Inc., Argent Chemical Laboratories Inc., Redmond, WA, USA) which was buffered with sodium bicarbonate. Once a fish was unresponsive, it was transferred to a fish holder in a 10 L surgery tray (Fig. 2A). Throughout surgery, fresh oxygenated water containing a dilute amount of MS-222 (0.082 g l^{-1} of MS-222 at 15 ± 1 °C) was recirculated over the fish gills through a small tube inserted in the fish's mouth (Fig. 2B). A scalpel was used to remove the skin over the cranium and a Dremel (Dremel, WI, USA) slowly removed bone until the cranial cavity was exposed (Vinepinksy et al., 2017) (Fig. 2B). The amplifier and ribbon jumpers were then anchored to the body with a series of sutures anterior to the dorsal fin (4–0·gauge braided silk thread; Ethicon Inc., Somerville, NJ, USA) (Fig. 2D). The reference electrode was placed in the cerebrospinal fluid of the brain and recording electrodes were then inserted into target regions of the brain (e.g. the cerebellum and optic tectum) with micro-forceps (Fine Scientific Tools, CA, USA) (Fig. 2C). To confirm electrode placement in the brain, cerebellar activity was monitored during light swimming bouts in the surgery tray under a lower dosage of MS-222. If no neural activity was then observed, electrodes were repositioned. Once electrode placement was finalized, dental cement (3 M, MN, USA) was applied dental to form a small, hollow dome over the cranial cavity so that brain was not in contact with the dental cement itself. This locked the electrodes in place and sealed the brain from the external environment (Fig. 2D). After surgery (~40 min), fish were transferred to a 10 L tank with fresh oxygenated water and allowed to recover until a righting response was observed. Fish were then transferred to the working area of the flow tank and acclimated for 25 min before experimentation started. After experimentation, fish were euthanized with MS-222 and electrodes were surgically removed to confirm placement.

A similar setup was used for toadfish. Fish were anesthetized in 10 L tank (20 ± 1 °C) containing our MS-222 solution (0.164 g l^{-1}). Since toadfish have a compressed, flattened body, fish rested on submerged foam mat (20 ×15 cm) during surgery.

2.6. Experimentation

Trout and toadfish were placed in a variable speed flow tank (850 L, Loligo systems, Denmark) and were subjected to uni-directional, uniform flow (Taguchi and Liao, 2011; Akanyeti et al., 2017). After acclimating for 25 min, a low flow speed (11 cm/s) was introduced to induce rheotactic behaviors to orient fish against the current. Once a fish was oriented upstream, the flow speed was increased to encompass a range of swimming speeds (28 cm/s to 70 cm/s).

In addition to flow stimuli, we exposed fish to various visual stimuli consisting of 1) single or multiple bursts of visible light from an LED source located laterally, 2) a looming stimulus and 3) the silhouette of a prey particle. In the case of the looming and prey stimuli, a short throw projector (Brightlink 696Ui, Epson, Japan) was used to project images dorsally to the fish. A custom MATLAB script generated looming stimuli at various expansion rates and prey trajectories at constant velocities. All experiments were conducted with the room lights turned off.

Amplifier outputs were filtered (60 Hz notch filter, 300 Hz low, 5000 Hz high cutoff) and recorded with the software LabChart (20 kSPS; AD Instruments Ltd, Dunedin, NZ). High-speed video (150 fps, Phantom Miro 340 high speed, Vision Research, Wayne, NJ, USA) aimed at a front surface mirror below the flow tank captured swimming kinematics

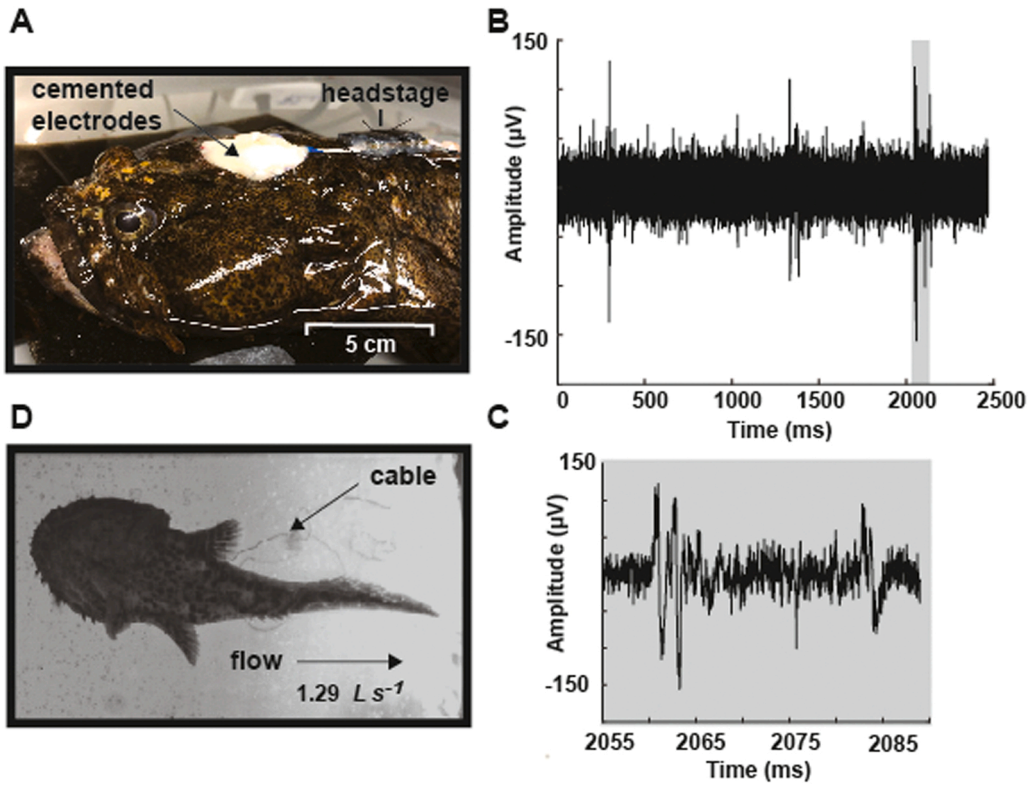

Fig. 5. Electrode implantation (A) and example recording (B,C) from the tethered amplifier in a marine toadfish (*Opsanus tau*) cerebellum in uniform flow (D, 1.29 Ls^{-1}).

(Fig. 3A). Neural and video recordings were synchronized using an external trigger that directly interfaced to the data acquisition system and high-speed cameras.

3. Results

3.1. Behavior of fish swimming in flow

Rainbow trout with the attached amplifier exhibited exploratory swimming behaviors at low flow speeds and bursts of acceleration at higher flow speeds (1.0–2.4 $L\ s^{-1}$), similar to control trout with no tether. All fish with the amplifier also exhibited stereotypical, C-start escape responses to expanding loom stimuli (Peek and Card, 2016; Hein et al., 2018) (Supplemental Figure 1A). In addition to responding to negative stimuli that elicited escapes, we also presented positive prey stimuli that elicited attacks, even with the amplifier attached. Feeding attacks would sometimes occur as quickly as 5 min from the initial stimuli presentation(Supplemental Figure 1B).

To demonstrate the applicability of our system to marine habitats, we implanted electrodes into a saltwater toadfish. Toadfish were also subjected to a range of swimming speeds (0.4–2.0 $L\ s^{-1}$). Because toadfish are demersal, sedentary fishes, they did not respond readily to loom or prey stimuli. Instead, they responded best to computer-controlled flow accelerations. The ability of fish to demonstrate natural aversive and attractive behaviors give us confidence that our recording approach can be applied to a diversity of natural behaviors.

3.2. Recordings from freely behaving rainbow trout and toadfish

We obtained extracellular recordings from the cerebellum of trout swimming at various speeds. Simultaneous high-speed video of the swimming kinematics revealed the motor activity of the cerebellum. We observed that the cerebellum was active only during specific times during the tailbeat cycle. For example, a cerebellar recording from an individual (BL=29.8 cm) swimming at 28 cm/s (0.94 $L\ s^{-1}$) showed that the neurons in the close proximity of our electrodes were active during the lateral-most excursion of the tail beat cycle (Fig. 4). Experiments could last several hours, and thus recordings have the potential to be continuously monitored for longer durations.

Extracellular recordings from the cerebellum in toadfish were obtained when fish burst forward in response to flow velocity fluctuations (Fig. 5). Recordings from toadfish were much shorter overall (~30 min) because of the innate behavior of the species. Toadfish would commonly spin about their long axis which created excessive tension on the electrodes. In addition, prolonged spinning tangled and kinked the output cable, causing damage that necessitated fabricating another replacement.

To validate the consistency of our system across different regions of the CNS, we recorded activity in the optic tectum (OT) of trout. We observed multi-unit activity in the OT following exposure to single and multiple bursts of light from an LED flashlight (Fig. 6).

4. Discussion

4.1. Brain activity in freely swimming adult fishes

Here we developed an approach to record real-time neural activity in freely moving adult fishes. Brain activity in adult fishes is often investigated through immediate early gene (IEGs) expression. These genes, such as *c-fos* and *erg-1*, express proteins in response to neuronal activity or external stressors. IEG expression, revealed through immunohistochemical techniques, has been critical to our understanding of social behaviors (Maruska and Fernald, 2011; Fernald and Maruska, 2012) such as when *erg-1* is expressed in male cichlids ascending in social status (Burmeister et al., 2005). These studies have revolutionized our ability to understand the activity of specific brain regions in naturally behaving animals, but also require post-mortem dissection and cannot resolve the neural activity of behaviors in real-time. Complex behaviors

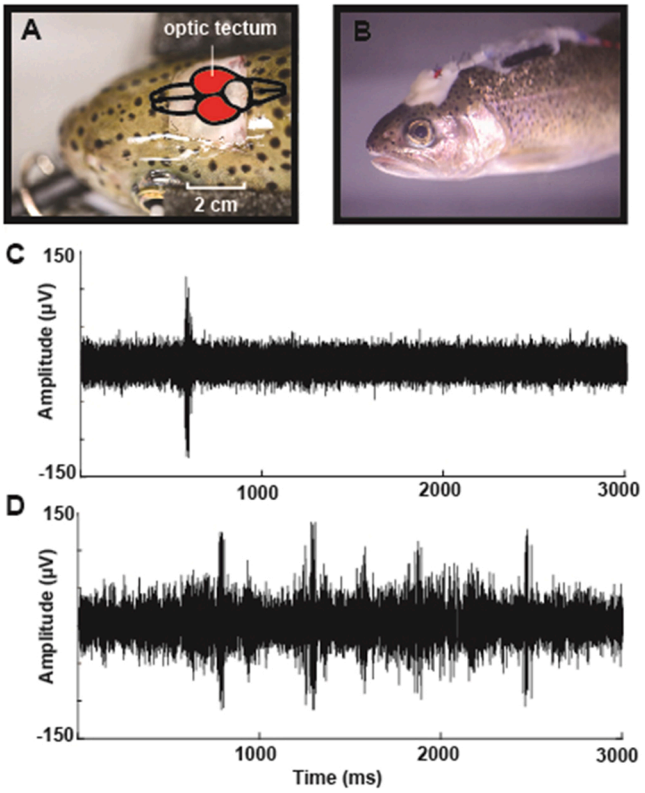

Fig. 6. Multi-unit extracellular recording from the optic tectum of a rainbow trout swimming in flow (1.3 Ls^{-1}). (A) Electrodes were surgically implanted into the optic tectum. (B) Once fish recovered and were freely swimming in the flow tank, they were presented with visual stimuli from an LED light source. Typical optic tectum responses from single (C) and multiple bursts of light (D).

are typically composed of discrete, sequential steps culminating in a final behavioral outcome. Since each discrete step likely requires a specific subset of neurons, only by observing the neural activity of these behaviors as they occur can we elucidate the temporal patterns of dedicated neuronal populations. This is best exemplified by the powerful optical and genetic advances in larval zebrafish (Kim et al., 2017), where real time, brain-wide activity with cellular resolution in moving animals can be achieved. These approaches require species with well-classified genomes to genetically encode fluorescence, which, while becoming more accessible (Gratacap et al., 2020), is currently challenging for comparing neural activity across species. Functional fluorescent imaging approaches rely on larval fish due to their body transparency, but this approach has also been applied to transparent adult species such as *Danionella translucida* (Schulze et al., 2018). Functional fluorescent imaging in adult fishes promises to further our understanding of more complex behaviors but these studies are limited to small fields of view as imaging can only resolve surface regions of the brain. Our approach encourages comparative studies in adult fishes, as our amplifier can be potentially used to monitor neural signals in any region of the brain in a diversity of wild species.

4.2. Neural recordings in flowing water

Our motivation to build a streamlined neural recording system was to access the neural basis of natural swimming behaviors. A previous study developed wireless recordings for freely swimming goldfish (*Carassius auratus*) and found that the neurons of the lateral pallium may constitute the building blocks of the fish navigation system (Vinepinksy et al., 2020). Vinepinksy's pioneering study was designed to investigate place cells in the fish brain, with less emphasis on the natural ecology of fish behaviors. Our amplifier has the unique hydrodynamic advantage of permitting recordings from a larger selection of species and behaviors.

Fish live in complex hydrodynamic environments where they must continually sense and adapt to ever-changing environmental flows. Stability in turbulence undoubtedly requires neural feedback mechanisms, and yet despite this fact, no neural recordings exist of freely swimming fish in turbulent flow regimes. Because zebrafish are small, swimming studies are restricted to flow regimes at low Reynolds numbers, where the ratio of inertial to viscous forces are low (Vanwalleghem et al., 2020). However, at higher Reynolds numbers flow becomes turbulent and is dominated by eddies of multiple scales. These turbulent conditions have been shown to influence both fish behavior (Liao et al., 2003; Liao, 2007; Tritico and Cotel, 2010; Cotel and Webb, 2015) and energetics (Enders et al., 2003; Enders et al., 2005; Taguchi and Liao, 2011). Our streamlined electrophysiology amplifier is poised to reveal the neural circuitry underlying movement and navigation through unsteady flows. For example, recordings of the VIII nerve and the medial octavolateral nucleus could advance our understanding of how lateral line hair cells can distinguish prey from background noise while the body is moving (Pohlmann et al., 2004; Chagnaud et al., 2006; Chagnaud et al., 2007). In fishes, locomotion generates fluid-structure interactions that require the animal to both sense and respond to fluid forces acting upon the body. Our approach can be used to help understand how the neuromuscular system integrates sensory information in real-time to produce adaptive motor outputs.

4.3. Applications for a low-cost neural recording setup

While recordings from freely moving animals in the laboratory can generate novel insights into the neural circuitry of sensory processes, higher-order social interactions require large spaces for uninhibited behaviors. Our setup can also be adapted with a data logger to permit wireless recordings in large mesocosms and even the field. Social behaviors from bats to macaques have been shown to drastically influence brain activity (Báez-Mendoza et al., 2013; Báez-Mendoza et al., 2021; Rose et al., 2021) such as how hippocampal neurons in bats encode the presence of conspecifics during social flying behaviors (Omer et al., 2018). Like collectively flying bats, schooling fish must also coordinate movement to navigate as acohesive group. Our recording system can be applied to uncover the neural activity of these and other complex social behaviors in large mesocosms. For example, a 16-channel recording from across the fish cerebellum could reveal how premotor neurons are distributed, reminiscent of the spatial organization of neurons responsible for reaching and grasping in the primate brain (Carmena et al., 2003). Additionally, brain recordings of multiple individuals during schooling could help elucidate which brain regions are responsible for encoding the presence of conspecifics. Since social behaviors are not limited to conspecifics, our setup can also be utilized to record the brain activity of predators and prey as they interact with one another.

Some behaviors cannot be observed in manmade mesocosms due to large species size or environments that are difficult to replicate (e.g. deeper oceanic zones). Our understanding of how wild animals move and behave has expanded greatly with the advent of electronic tags, which have provided unprecedented insights into natural behaviors from lobsters to whales (Jury et al., 2018; Czapanskiy et al., 2022). For example, Atlantic bluefin tuna have been shown to maintain warm body temperatures even when diving to depths >1000 m (Block et al., 2001). Tagged white sharks have revealed energy-efficient gliding behavior during foraging that leads to increased net energy gains (Watanabe et al., 2019). Coupling the ability to record from brain regions dedicated to sensory modalities or physiological states would amplify our understanding of pelagic animal behaviors. Converting our low-cost amplifier (~ $70) into a data logger and coupling it with existing technologies opens up exciting opportunities for monitoring neural activity in the wild. For example, neural recordings of the optic tectum paired with a depth sensor could help us understand how the visual system is used by swordfish in deep sea, low-light conditions. In combination with satellite

telemetry, one could also monitor stress levels through the preoptic hypothalamic nucleus (Wendelaar Bonga, 1997; Flik et al., 2006) as coastal fish move through anthropogenic zones or waters effected by climate change.

By providing a low-cost underwater electrophysiology setup, we hope that our results will encourage future investigations of neural activity across a range of aquatic animals (e. g., cephalopods, mammals and reptiles) in both the lab and the field.

Funding

This work was supported by the National Science Foundation (Grant IOS 1856237 and IOS 2102891) to J.C.L.

All experimental procedures were approved IUACUC (ID 202200000056).

Author Contributions

B.J.G., J.A.S., J.C.L. Conceptualization, B.J.G., J.A.S., J.C.L. Methodology, B.J.G., J.A.S. Validation, B.J.G. J.A.S. Formal analysis, B.J.G., J.C.L Investigation, J.A.S., J.C.L. Resources, B.J.G. Data curation, B.J.G. Writing - original draft, B.J.G., J.A.S., J.C.L. Writing - review & editing,J.C.L. Supervision,J.C.L. Project administration, J.C.L. Funding acquisition.

Declaration of Competing Interest

None.

Data availability

Data will be made available on request.

Acknowledgements

We thank E. Vinepinksy and R. Segev for sharing valuable insights throughout the process, K. Otto for assistance and feedback in electrode selection, and A. Hein and B. Martin for help with the visual stimulus setup.

Appendix A. Supporting information

Supplementary data associated with this article can be found in the online version at doi:10.1016/j.jneumeth.2023.109850.

References

Agnew, W.S., Levinson, S.R., Brabson, J.S., Raftery, M.A., 1978. Purification of the tetrodotoxin-binding component associated with the voltage-sensitive sodium channel from Electrophorus electricus electroplax membranes. PNAS 75, 2606–2610.
Ahrens, M.B., Orger, M.B., Robson, D.N., Li, J.M., Keller, P.J., 2013. Whole-brain functional imaging at cellular resolution using light-sheet microscopy. Nat. Methods 10, 413–420.
Akanyeti, O., Putney, J., Yanagitsuru, Y.R., Lauder, G.V., Stewart, W.J., Liao, J.C., 2017. Accelerating fishes increase propulsive efficiency by modulating vortex ring geometry. PNAS 114, 13828–138333.
Báez-Mendoza, R., Harris, C.J., Schultz, W., 2013. Activity of striatal neurons reflects social action and own reward. PNAS 110, 16634–16639.
Báez-Mendoza, R., Mastrobattista, E.P., Wang, A.J., Williams, Z.M., 2021. Social agent identity cells in the prefrontal cortex of interacting groups of primates. Science 374.
Block, B.A., Dewar, H., Blackwell, S.B., Williams, T.D., Prince, E.D., 2001. Migratory movements, depth preferences, and thermal biology of Atlantic bluefin tuna. Science 293, 1310–1314.
Broglio, C., Rodriguez, F., Salas, C., 2003. Spatial cognition and its neural basis in teleost fishes. Fish Fish 4, 247–255.
Brown, C., Laland, K., Krause, J., 2006. Fish Cognition and Behavior, Fish and Aquatic Resources Series 11. Blackwell Publishing,.
Burmeister, S.S., Jarvis, E.D., Fernald, R.D., 2005. Rapid behavioral and genomic responses to social opportunity. PLoS Biol. 3.
Canfield, J.G., Mizumori, S.J.Y., 2004. Methods for chronic neural recording in the telencephalon of freely behaving fish. J. Neurosci. Methods 133, 127–134.
Carmena, J.M., Lebedev, M.A., Crist, R.E., O'Doherty, J.E., Nicolelis, M.A.L., 2003. Learning to control a brain–machine interface for reaching and grasping by primates. PLoS Biol. 1, 193–208.
Catterall, W.A., 1988. Structure and function of voltage-sensitive ion channels. Science 242, 50–61.
Chagnaud, B.P., Bleckmann, H., Engelmann, J., 2006. Neural responses of goldfish lateral line afferents to vortex motions. J. Exp. Biol. 209, 327–342.
Chagnaud, B.P., Hofmann, M.H., Mogdans, J., 2007. Responses to dipole stimuli of anterior lateral line nerve fibres in goldfish, Carassius auratus, under still and running water conditions. J. Comp. Physiol. A 193, 249–263.
Cotel, A.J., Webb, P.W., 2015. Living in a turbulent world—a new conceptual framework for the interactions of fish and eddies. Integr. Comp. Biol. 55, 662–672.
Crapse, T.B., Sommer, M.A., 2008. Corollary discharge across the animal kingdom. Nat. Rev. Neurosci. 9, 587–600.
Czapanskiy, M.F., Poganis, P.J., Fahlbusch, J.A., Schmitt, T.L., Goldbogen, J.A., 2022. An accelerometer-derived ballistocardiogram method for detecting heart rate in free-ranging marine mammals. J. Exp. Biol. 225.
Daw, N.W., 1968. Colour-coded ganglion cells in the goldfish retina: extension of their receptive fields by means of new stimuli. J. Physiol. 197, 567–592.
Enders, E.C., Boisclair, D., Roy, A.G., 2003. The effect of turbulence on the cost of swimming for juvenile Atlantic salmon (Salmo salar). Can. J. Fish. Aquat. Sci. 60, 1149–1160.
Enders, E.C., Boisclair, D., Roy, A.G., 2005. A model of total swimming costs in turbulent flow for juvenile Atlantic salmon (Salmo salar). Can. J. Fish. Aquat. Sci. 62, 1079–1089.
Evarts, E.V., 1968. Relation of pyramidal tract activity to force exerted during voluntary movement. J. Neurophysiol. 31, 14–27.
Fernald, R.D., Maruska, K.P., 2012. Social information changes the brain. PNAS 109, 17194–17199.
Flik, G., Klaren, P.H.M., Van den Burg, E.H., Metz, J.R., Huising, M.O., 2006. CRF and stress in fish. Gen. Comp. Endocrinol. 146, 36–44.
Girotti, M., Pace, T.W., Gaylord, R.I., Rubin, B.A., Herman, J.P., Spencer, R.L., 2006. Habituation to repeated restraint stress is associated with lack of stress-induced c-fos expression in primary sensory processing areas of the rat brain. Neuroscience 138, 1067–1081.
Gratacap, R.L., Regan, T., Dehler, C.E., 2020. Efficient CRISPR/Cas9 genome editing in a salmonid fish cell line using a lentivirus delivery system. BMC Biotechnol. 20.
Hein, A.M., Gil, M.A., Twomey, C.R., Levin, S.A., 2018. Conserved behavioral circuits govern high-speed decision-making in wild fish shoals. PNAS 115, 12224–12228.
Juczewski, K., Koussa, J.A., Kesner, A.J., Lee, J.O., Lovinger, D.M., 2020. Stress and behavioral correlates in the head-fixed method: stress measurements, habituation dynamics, locomotion, and motor-skill learning in mice. Sci. Rep. 10.
Jury, S.H., Langley, T., Gutzler, B.C., Goldstein, J.S., Watson, W.H., 2018. Monitoring the behavior of freely moving lobsters with accelerometers. Bull. Mar. Sci. 94, 533–553.
Kim, D.H., Kim, J., Marques, J.C., Grama, A., Hildebrand, D.G., Gu, W., Li, J.M., Robson, D.N., 2017. Pan-neuronal calcium imaging with cellular resolution in freely swimming zebrafish. Nat. Methods 14, 1107–1114.
Liao, J.C., 2007. A review of fish swimming mechanics and behaviour in altered flows. Philos. Trans. R. Soc. B: Biol. Sci. 362, 1973–1993.
Liao, J.C., Beal, D.N., Lauder, G.V., Triantafyllou, M.S., 2003. Fish exploiting vortices decrease muscle activity. Science 302, 1566–1569.
Maruska, K.P., Fernald, R.D., 2011. Social regulation of gene expression in the hypothalamic-pituitary-gonadal axis. Physiology 26, 412–423.
Musall, S., Kaufman, M.T., Juavinett, A.L., Gluf, S., Churchland, A.K., 2019. Single-trial neural dynamics are dominated by richly varied movements. Nat. Neurosci. 22, 1677–1686.
Noda, M., Shimizu, S., Tanabe, T., Takai, T., Kayano, T., Numa, S., 1984. Primary structure of Electrophorus electricus sodium channel deduced from eDNA sequence. Nature 312, 121–127.
Omer, D.B., Maimon, S.R., Las, L., Ulanovsky, N., 2018. Social place-cells in the bat hippocampus. Science 359.
Palmer, L.M., Giuffrida, B.A., Mensinger, A.F., 2003. Neural recordings from the lateral line in free-swimming toadfish, *Opsanus tau*. Biol. Bull. 205, 216–218.
Peek, M.Y., Card, G.M., 2016. Comparative approaches to escape. Curr. Opin. Neurobiol. 41, 167–173.
Philip, R.L., Parker, Morgan, Brown, A., Matthew, C., Smear, Cristopher, Niell, M., 2020. Movement-related signals in sensory areas: roles in natural behavior. Trends Neurosci. 43, 581–595.
Pohlmann, K., Atema, J., Breithaupt, T., 2004. The importance of the lateral line in nocturnal predation of piscivorous catfish. J. Exp. Biol. 207, 2971–2978.
Prutchi, D., Norris, M., 2005. Design and Development of Medical Electronic Instrumentation. Wiley-Interscience,.
Rose, M.C., Styr, B., Schmid, T.A., Elie, J.E., Yartsev, M.M., 2021. Cortical representation of group social communication in bats. Science 374.
Rynes, M.L., Surinach, D.A., Linn, S., Kodandaramaiah, S.B., 2021. Miniaturized head-mounted microscope for whole-cortex mesoscale imaging in freely behaving mice. Nat. Methods 18, 417–425.
Schreier, L.A., 1978. Electrostatic Damage Susceptibility of Semiconductor Devices. 16th International Reliability Physics Symposium 151–153.
Schulze, L., Henninger, J., Kadobianskyi, M., Judkewitz, B., 2018. Transparent Danionella translucida as a genetically tractable vertebrate brain model. Nat. Methods 15, 977–983.
Skandalis, D.A., Lundsford, E.T., Liao, J.C., 2021. Corollary discharge enables proprioception from lateral line sensory feedback. PLOS Biol. 19.
Taguchi, M., Liao, J.C., 2011. Rainbow trout consume less oxygen in turbulence: the energetics of swimming behaviors at different speeds. J. Exp. Biol. 214, 1428–1436.

Takahashi, S., Hombe, T., Takahashi, R., Ide, K., Okamoto, S., Yoda, K., Kitagawa, T., Makiguchi, Y., 2021. Wireless logging of extracellular neuronal activity in the telencephalon of free-swimming salmonids. Anim. Biotelemetry 9.
Tritico, H.M., Cotel, A.J., 2010. The effects of turbulent eddies on the stability and critical swimming speed of creek chub (*Semotilus atromaculatus*). J. Exp. Biol. 213, 2284–2293.
Turner, R.S., DeLong, M.R., 2000. Corticostriatal activity in primary motor cortex of the macaque. J. Neurosci. 20, 7096–710.
Vanwalleghem, G., Shuster, K., Taylor, M.A., Favre-Bulle, I.A., Scott, E.K., 2020. Brain-Wide Mapping of Water Flow Perception in Zebrafish. J. Neurosci. 40, 4130–4144.
Vinepinksy, E., Donchin, O., Segev, R., 2017. Wireless electrophysiology of the brain of freely swimming goldfish. Journal of Neuroscience Methods 278, 76–86.
Vinepinksy, E., Cohen, L., Perchik, S., Ben-Shahar, O., Donchin, O., Segev, R., 2020. Representation of edges, head direction, and swimming kinematics in the brain of freely-navigating fish. Sci. Rep. 10, 1–16.
Watanabe, Y.Y., Payne, N.L., Semmens, J.M., Fox, A., Huveneers, C., 2019. Swimming strategies and energetics of endothermic white sharks during foraging. J. Exp. Biol. 222.
Weiss, S.A., Zottoli, S.J., Do, S.C., Faber, D.S., Preuss, T., 2006. Correlation of C-start behaviors with neural activity recorded from the hindbrain in free-swimming goldfish (Carassius auratus). J. Exp. Biol. 209, 4788–4800.
Wendelaar Bonga, S.E., 1997. The stress response in fish. Physiol. Rev. 77, 591–625.
Yartsev, M.M., Ulanovsky, N., 2013. Representation of three-dimensional space in the hippocampus of flying bats. Science 340, 367–372.